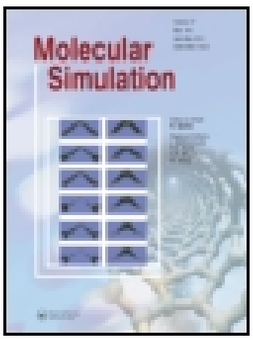

Molecular Simulation

ISSN: 0892-7022 (Print) 1029-0435 (Online) Journal homepage: http://www.tandfonline.com/loi/gmos20

First principles study of the electronic structure and optical properties of chrysene under pressure

Lingping Xiao, Li Zeng & Xue Yang

To cite this article: Lingping Xiao, Li Zeng & Xue Yang (2018): First principles study of the electronic structure and optical properties of chrysene under pressure, Molecular Simulation

To link to this article: https://doi.org/10.1080/08927022.2018.1547819

Published online: 22 Nov 2018.

MOLECULAR SIMULATION
https://doi.org/10.1080/08927022.2018.1547819

Taylor & Francis
Taylor & Francis Group

First principles study of the electronic structure and optical properties of chrysene under pressure

Lingping Xiao[a], Li Zeng[b] and Xue Yang[c]

[a]Jiangxi Science and Technology Normal University, Nanchang, People's Republic of China; [b]Jiangxi Hongdu Aviation Industry Group Corporation Limited, Nanchang, People's Republic of China; [c]Key Laboratory of Materials Physics, Institute of Solid State Physics, Chinese Academy of Sciences, Hefei, People's Republic of China

ABSTRACT

Structural parameters, electronic and optical properties of chrysene have been investigated using the plane-wave ultrasoft pseudopotential technique based on the first principles density functional theory. The pressure dependence of the electronic band structure, density of states and partial density of states of chrysene were presented. Meanwhile, the complex dielectric function, refractive index, absorption coefficient, reflectivity, and the extinction coefficient are calculated and analysed. According to our work, we found that the optical properties of chrysene undergo a red shift with increasing pressure.

ARTICLE HISTORY
Received 9 May 2018
Accepted 6 November 2018

KEYWORDS
Polycyclic aromatic hydrocarbons; density functional theory; high pressure; chrysene

1. Introduction

Organic molecular solids have attracted considerable interest for both fundamental reasons and possible technological applications. Recently, organic molecular solids have attracted significant attention owing to their proposed applications in (opto)electronic devices such as field-effect transistors, light-emitting diodes and photovoltaic cells [1–4]. Moreover, due to the relatively weak intermolecular interaction of organic molecular solids, the characteristic of these solids is very responsive to applied pressure [5]. In some cases, this has resulted in intriguing and unexpected physical properties, such as metallic behaviour [6] and superconductivity [7,8].

Chrysene was chosen for this study, as a representative of the large class of polycyclic hydrocarbons that have served for a long time as model compounds for organic molecular crystals. At ambient pressure and room temperature, pure chrysene crystal structure belongs to the monoclinic has space group $I2/c$ with four molecules in the primitive unit cell [9]. The molecules arrange in a herringbone manner which is typical for many aromatic hydrocarbon molecular solids and can be seen as a consequence of the densest possible packing of the molecules within the crystal with the least possible repulsion [10]. While these fascinating material properties have attracted much attention, many theoretical investigations have provided the first insight into the electronic properties of chrysene. Earlier studies revealed that each carbon forms three covalent σ bonds, the fourth valence electron stays in a $2p$ orbital perpendicular to the molecular plane generating the π-electron cloud [11]. The electronic and optical properties of compounds with two to five aromatic rings, using first principle methods, were studied by Hummer et al. [12]. F. Roth et al. have investigated the electronic properties of chrysene molecular solids by performed electron energy-loss spectroscopy in transmission [10]. These theoretical calculations were suggested that first principle studies of the electronic properties under pressure and obtaining equation of state of chrysene are possible. Moreover, pressure as one of the fundamental state parameters can be used to tune the lattice and electronic structure efficiently, which alters the structural and magnetic ordering. In order to gain a deeper understanding of the relationship between the geometric structure, and electrical properties behaviour as well as optical properties in molecular materials should promote advancement of functional organic devices. Here, we examine the pressure dependent geometrical and electronic properties of chrysene under hydrostatic pressure up to 9 GPa. The information of the pressure dependence of lattice parameters, the band structure, the total density of states (DOS) and partial density of states (PDOS) are provided. Meanwhile, the complex dielectric function, refractive index, absorption coefficient, reflectivity, and the extinction coefficient are calculated.

2. Calculation method

The calculations carried out in this work are based on the density functional theory (DFT) using the VASP program package [13]. The geometric structure was fully optimised using DFT with the generalised gradient approximation with van der Waals interactions treated using the vdW-DF2 correlation functional [14]. Moreover, the dispersive interaction between atoms and molecules is important for many molecular and solid structures. The vdW-DF2 method and the semi-empirical DFT method of Grimme (DFT-D2) [15], as well as the opt-B88-vdW method are successfully applied to several systems [16,17]. While more and more studies suggest that a many body approach is necessary for the realistic calculation of the

CONTACT Lingping Xiao xiaolingping1982@163.com

intermolecular cohesive energies, the vdW-DF2 method has been shown to reliably model the structures and energetics of organic molecular crystals under ambient and high-pressure conditions [18,19]. The self-consistent calculations were carried out with a $4 \times 3 \times$ k-point mesh. In this simulation, the ultrasoft pseudo-potentials are employed [20]. To balance accuracy and speed, the plane-wave basis set cutoff was set to 750 eV. The convergence criteria for total energy, max force, max tress, and SCF iterations were 5×10^{-6} eV/atom, 0.01 eV/Å, 0.02 GPa, and 5×10^{-7}eV/atom, respectively.

We adopt the experimental lattice parameters of chrysene with $a = 25.203$ Å, $b = 6.196$ Å, $c = 8.386$ Å and $\beta = 116.20°$, to build the initial crystal structure [10]. In this simulation, the pressure was increased in 1 GPa steps. During the geometry optimisation, the space group of the chrysene crystal has been constrained to *I*2/c. Thus, no structural phase transition will be considered in this study.

Moreover, the different band and electronic density to states can induce different dielectric response. The dielectric function $\varepsilon(\omega) = \varepsilon_1(\omega) + i\varepsilon_2(\omega)$ is an important function to describe the optical properties. Because the imaginary part $\varepsilon_2(\omega)$ is the pandect of optical properties, we use formula (1) to calculate the $\varepsilon_2(\omega)$ of chrysene. In the formula, the superscript c and v represent conduction and valence bands, respectively. $\hat{u}$ is the electric-field vectors of incident light field.

$$\varepsilon_2(\omega) = \frac{2e^2\pi}{\Omega\varepsilon_0}\sum_{k,v,c}|\psi_k^c|\hat{u}\times r|\psi_k^v|^2\delta(E_k^c - E_k^v - E) \quad (1)$$

The real part $\varepsilon_1(\omega)$ was calculated by the Kramers–Kronig relation (formula (2)). In the relation, p represents the principal value of the integral. The formula (1) and (2) show the $\varepsilon_1(\omega)$ and $\varepsilon_2(\omega)$ are the response of the incident light.

$$\varepsilon_1(\omega) = 1 + \frac{2}{\pi}p\int_0^\infty \frac{\omega'\varepsilon_2(\omega')}{\omega'^2 - \omega^2}\mathrm{d}\omega' \quad (2)$$

Optical constants are important in designing optical devices. We use the following three formulas (3)–(6) to calculate the optical constants: the absorption coefficient ($\alpha(\omega)$), reflectivity ($R(\omega)$), refractive index ($n(\omega)$) and extinction coefficient ($k(\omega)$) [21,22].

$$\alpha(\omega) = \sqrt{2}\left[\sqrt{\varepsilon_1(\omega)^2 + \varepsilon_2(\omega)^2} - \varepsilon_1(\omega)\right]^{1/2} \quad (3)$$

$$R(\omega) = \left|\frac{\sqrt{\varepsilon_1(\omega) + j\varepsilon_2(\omega)} - 1}{\sqrt{\varepsilon_1(\omega) + j\varepsilon_2(\omega)} + 1}\right|^2 \quad (4)$$

$$n(\omega) = \left[\sqrt{\varepsilon_1^2(\omega) + \varepsilon_2^2(\omega)} + \varepsilon_1(\omega)^{1/2}/\sqrt{2}\right] \quad (5)$$

$$k(\omega) = \left[\sqrt{\varepsilon_1^2(\omega) + \varepsilon_2^2(\omega)} - \varepsilon_1(\omega)\right]^{1/2}/\sqrt{2} \quad (6)$$

Table 1. Calculated and experimental structural data [10] of the crystal chrysene under zero pressure.

Method	a_0 (Å)	b_0 (Å)	c_0 (Å)	β(°)
GGA	26.149	6.395	9.244	116.82
LDA	21.963	5.851	9.224	114.29
vdW-DF2	25.065	6.017	8.321	115.61
Exp.	25.203	6.196	8.386	116.20

3. Results and discussion

3.1 Evolution of structural properties with pressure

At ambient conditions, chrysene in a monoclinic unit cell where molecules are arranged in a herringbone configuration in the *ab* plane and are stacked along the *c* axis (as shown in Figure 1). The optimised results of the primitive cell of pure chrysene are shown in Table 1. Experimental and other theoretical values are also listed. Based on the vdW-DF2 functional, the optimised crystal lattice parameters are obtained as $a = 25.065$ Å, $b = 6.017$Å, $c = 8.321$ Å, and $V = 1130.8$ Å^3. Though the lattice parameters were computed at zero temperature, it is obvious that the optimised geometry parameters are good agreement with experimental results, meaning that our calculation is reasonable.

Variations of the lattice parameters of chrysene with pressure are plotted in Figure 2. At first, the lattice parameters rapidly change under the external pressure up to 2 GPa, then they change more slowly. When applying a linear fitting in the whole pressure range, the linear compressibility of the lattice parameters a, b, and c is 0.13 GPa^{-1}, 0.056 GPa^{-1}, and 0.126 GPa^{-1} up to 9 GPa, respectively. And the value of the lattice constant a is reduced by 1.127 Å with an increase of the external pressure from 0 to 9 GPa, while b and c show a pressure dependence of $\Delta b = 0.575$Å and $\Delta c = 1.115$Å, respectively. The non-uniform pressure dependence of the lattice parameters may mean that the chrysene undergoes anisotropic compression. More interesting, the monoclinic angle increased by $\Delta\beta = 0.53$ in the same pressure region, which is may due to the reduction of the lattice parameters and the associated increase of the layer distance. This similar behaviour was often observed in aromatic compound such as anthracene [13], perylene [23] and naphthalene dimmers [24,25].

Moreover, by increasing pressure, the unit cell volumes are readily compressed. The variation of the unit cell volume for chrysene with pressure is shown in Figure 3. The bulk modulus B_0, as a parameter directly reflecting the hardness of material, is derived by calculating cell volumes at different pressures and fitting it using the Birch–Murnaghan equation of state as below: $P = (3/2)B_0[(V/V_0)^{-7/3} - (V/V_0)^{-5/3}] \times \{1 + (3/4)(B_0' - 4)[(V/V_0)^{-2/3} - 1]\}$, where B_0' is the derivative of bulk modulus and V_0 is the volume at ambient pressure [26]. At 9 GPa the volume compression is $V/V_0 = 82.3\%$. The bulk modulus at ambient pressure and temperature is $B_0 = 12.26$ GPa and its derivative is $B_0' = 7.08$. The low bulk modulus shows that the sample is easily to be compressed under pressure.

3.2 Band structures and density of states

Experimental investigations of the electronic properties of chrysene at high pressure are limited. Consequently, the aim of this part of the work is to understand the electronic band structure, partial density of states and the band gap under pressure. The calculated electronic band structure of chrysene

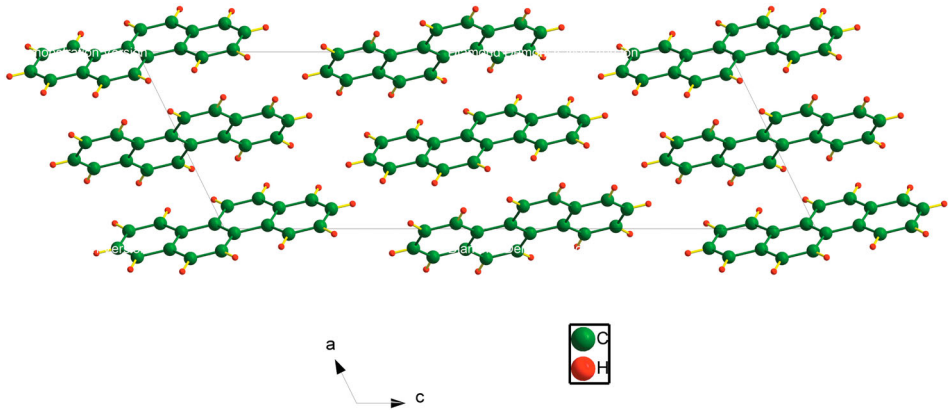

Figure 1. (Colour online) Crystal structure of chrysene. The red (green) spheres represent H (C) atoms.

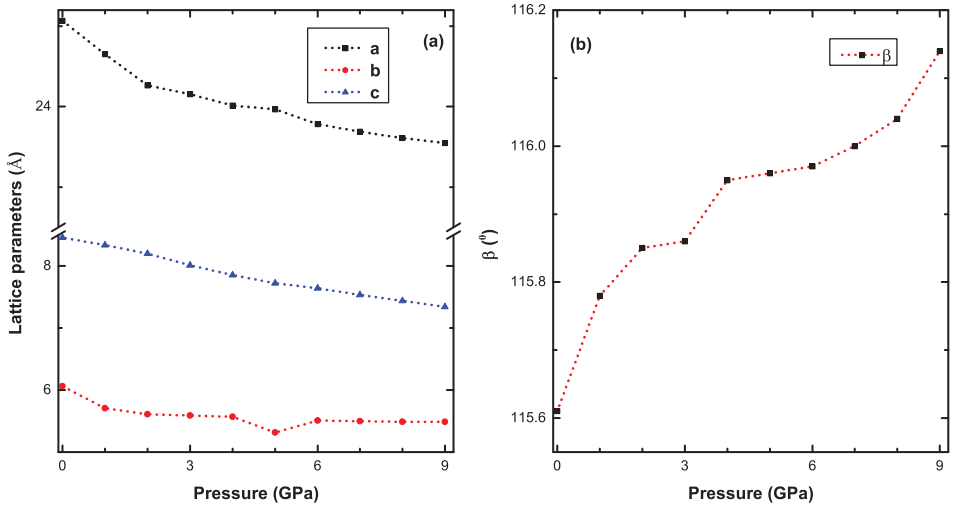

Figure 2. (Colour online) The lattice parameters of chrysene under high pressure up to 9 GPa.

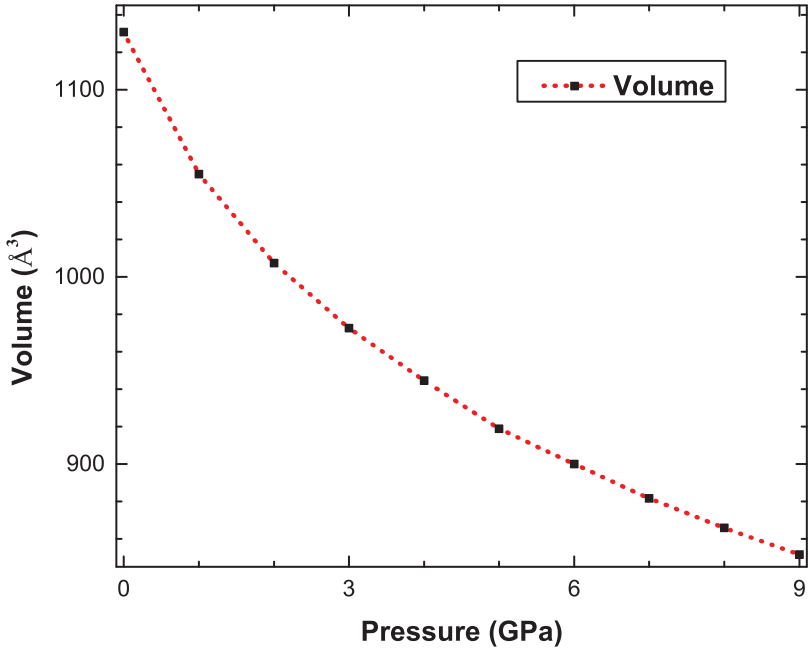

Figure 3. (Colour online) The unit cell volume compressibility of chrysene at zero temperature.

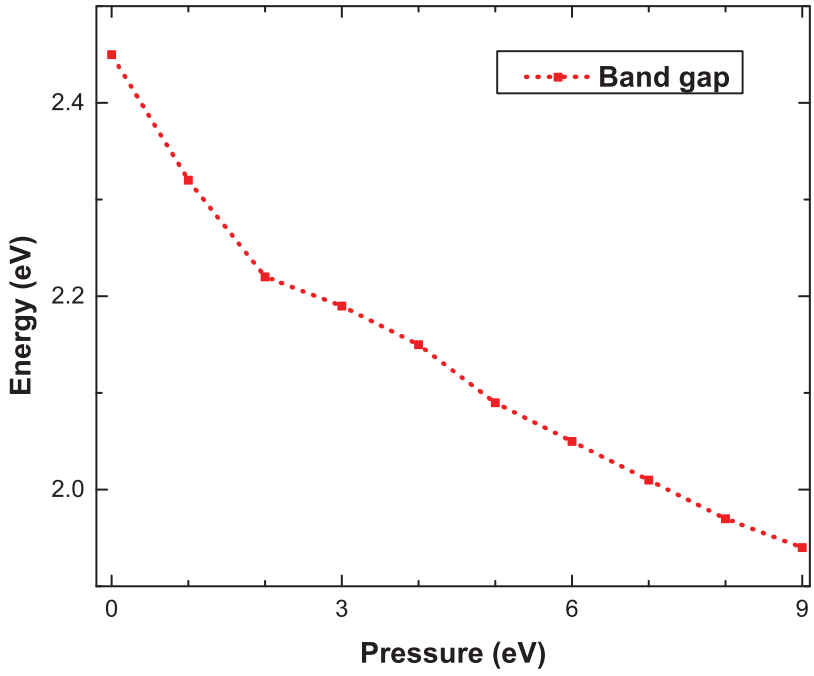

Figure 4. (Colour online) The band structures of chrysene at 0, 3, 6, and 9 GPa, respectively. The red dashed line is marked the Fermi level.

along with the high-symmetry points of the Brillouin zone is shown in Figure 4. The band structure calculations have been carried out following a path along the most high symmetry points L, M, A, G, Z, and V. The internal coordinates of these points are (−0.5, 0, −0.5), (−0.5, −0.5, −0.5), (−0.5, 0, 0), (0, 0, 0), (0, −0.5, −0.5), and (0, 0, −0.5) in the first Brillouin zone, respectively. As can be seen from Figure 4, the valence band maximum (VBM) and conduction band minimum (CBM) are located at same high symmetry G point. It means that chrysene is direct band gap semiconductor. We can see

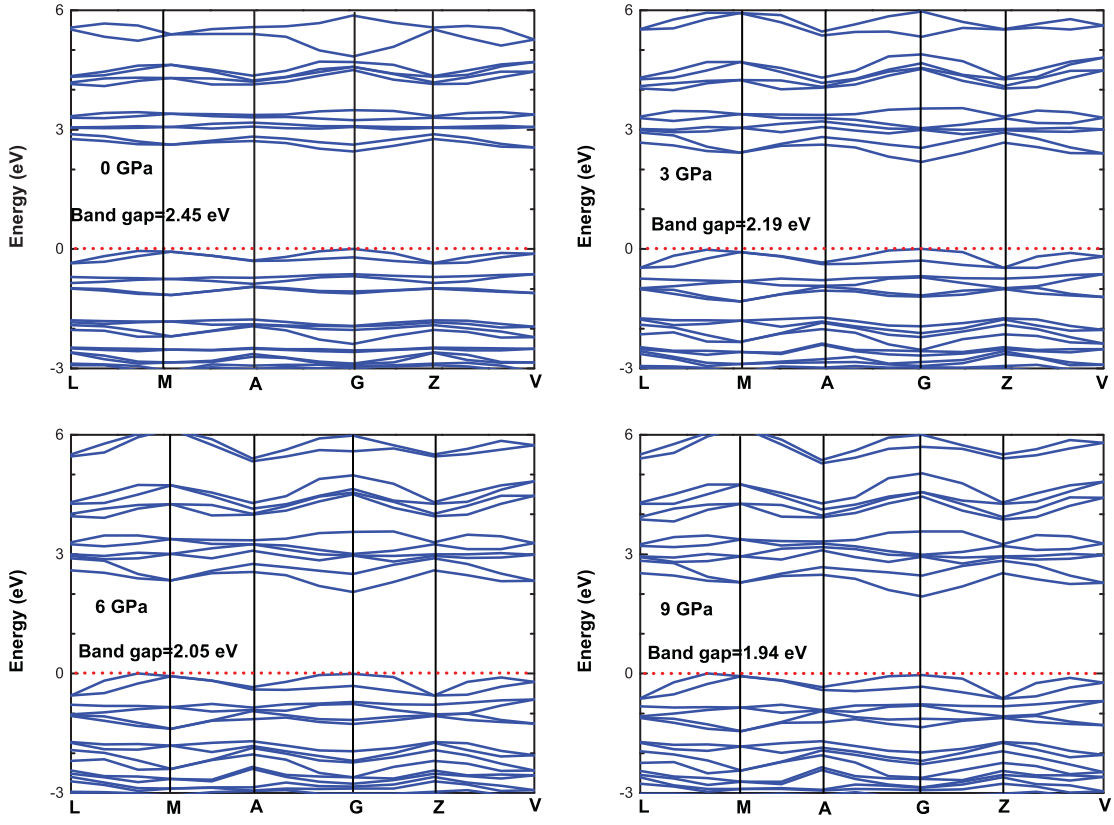

Figure 5. (Colour online) The density of state (PDOS) and partial density of state (PDOS) of chrysene at 0, 3, 6, and 9 GPa, respectively. The red dashed line is marked the Fermi level.

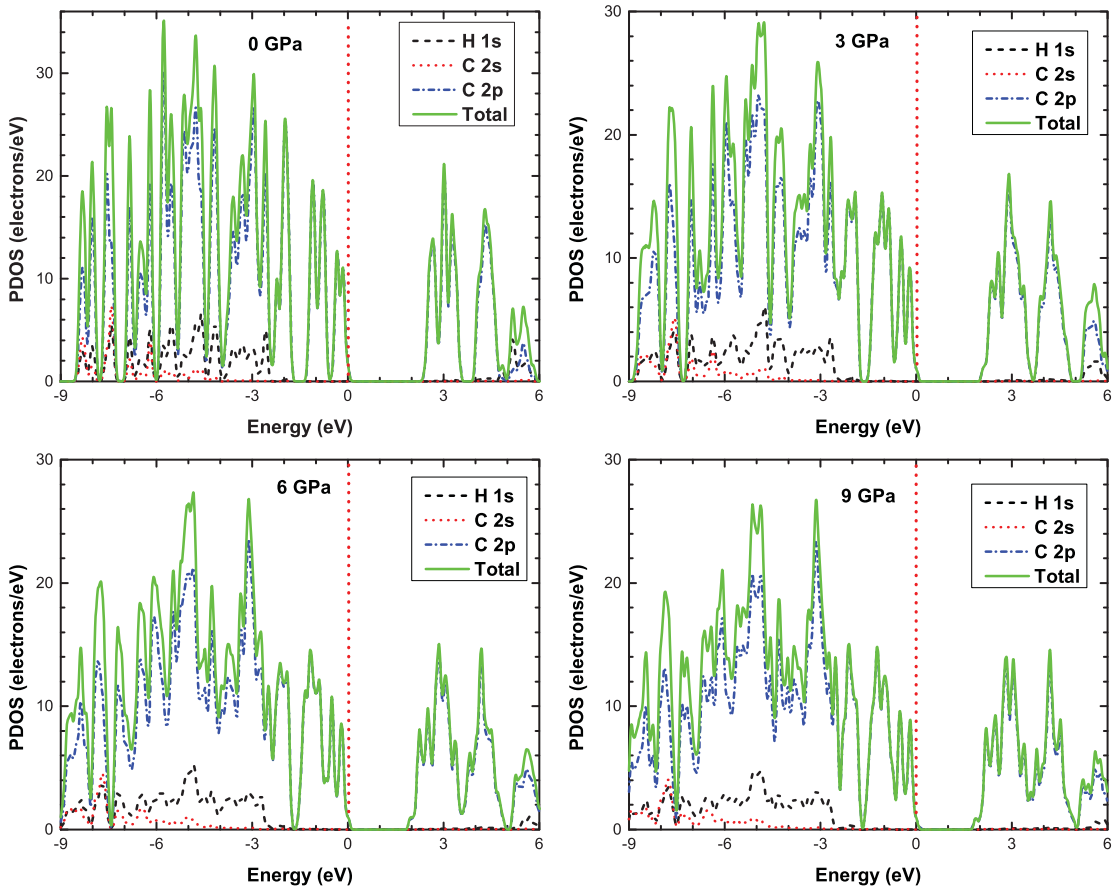

Figure 6. (Colour online) The dependence of the band gap of chrysene on pressure.

that a direct band gap is 2.45 eV, which is smaller than experimental data 3.3 eV due to the well-known underestimation of conduction band state energies in DFT calculations [27,28].

However, as the pressure increases, the conduction and valence band shift to lower and higher energies, respectively. The shifts of the conduction and valence band result in a decreasing band gap. Figure 4 shows the band gap of the chrysene under 3 GPa, 6 GPa, and 9 GPa are 2.19 eV, 2.05 eV, and 1.94 eV, respectively. The pressure dependence of the band gap is shown in Figure 5, clearly indicating the band gap decreases with increasing pressure. To determine the pressure coefficient, we fitted the direct band gap to determine the pressure coefficient, we fitted the direct band gap ($E_g(P)$) with a quadratic function: $E_g(P) = E_g(0)+aP + bP^2$, and obtained $a = -0.09$ eV/GPa and $b = 0.004$ eV/(GPa)^2.

To further elucidate the nature of the electronic band structure, the total density of states (DOS) and partial density of states (PDOS) of chrysene under 0 GPa, 3 GPa, 6 GPa, and 9 GPa are shown in Figure 6. According to the PDOS, the valence bands near the Fermi level between −2.37 and 0 eV mainly come from C 2p state and the band energy between −5.98 eV and −2.4 eV mainly derives from C 2p and H 1s states, while C 2s contributes little in this energy range. The valence band between −8.59 eV and −5.98 eV derives from C 2p and a strong hybridisation can be found between H 1s state and C 2s state in the valence band. The conduction band minimum is mainly composed of C 2p state. When increasing pressure, a slight shift of the peaks of PDOS for conduction and valence bands are shifted to lower and higher range. For example, the main peak of C 2p orbital in the valence band energy of chrysene shifts from −3.14 eV under a pressure of 3 GPa to −3.11 eV under a pressure of 6 GPa and then to −3.08 eV under a pressure of 9 GPa. The bottom of the conduction band shifts from 1.93 eV under a pressure of 3 GPa to 1.79 eV under a pressure of 6 GPa and then to 1.68 eV under a pressure of 9 GPa. As a result, the shifts of the conduction and valence band are consistent with the band structures.

3.3 Optical properties

We are interested in the effect of pressure on the optical properties. Figure 7 shows the reflectivity ($R(\omega)$), absorption coefficient ($\alpha(\omega)$), refractive index ($n(\omega)$) and the extinction coefficient ($k(\omega)$) at 0, 3, 6 and 9 GPa with photon energy ranging from 0 to 20 eV. From Figure 7, we can see that peaks of optical constants shift to lower energies with increasing pressure, which meaning undergo a red shift. As shown in Figure 7 (a), it is found that, at ambient pressure, the chrysene shows the strongest absorptive behaviour around the 5.11 eV. And the absorption coefficients further decrease rapidly in the high energy region. Additionally, the optical band gap of chrysene can be determined by the following relation: $(\alpha h\nu)^2 = A(h\nu - E_g)$, where A is a constant and E_g is the optical band gap, h is Planck's constant, and ν is the frequency of the incident photon [29]. The optical band gap was decreased from 2.45 to 1.94 eV as the pressure increase from 0 to

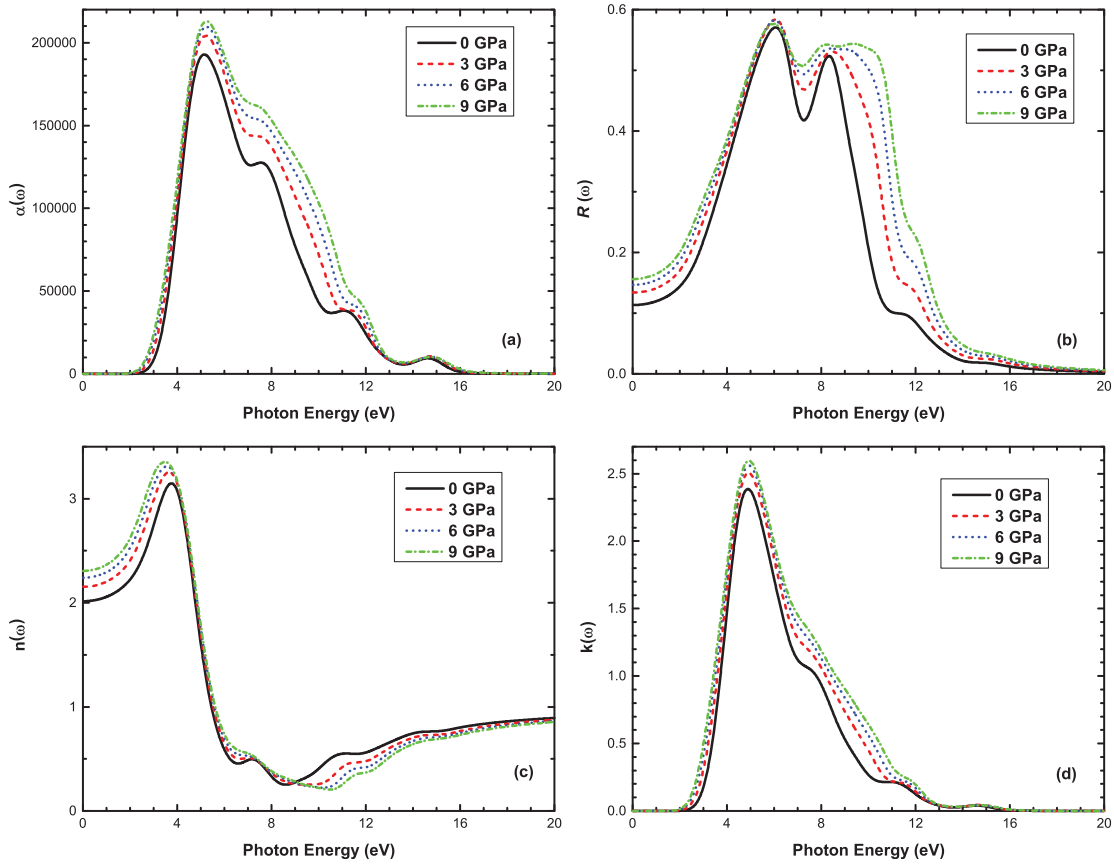

Figure 7. (Colour online) The optical constants of chrysene: (a) absorption coefficient ($\alpha(\omega)$); (b) reflectivity ($R(\omega)$); (c) the refractive index ($n(\omega)$); and (d) the extinction coefficient ($k(\omega)$).

9 GPa, which is consistent with the calculated band structures. Notably, the values of $R(\omega)$ of the main peak are at 6.08 eV, and 8.35 eV under normal pressure are shown in Figure 7(b). With pressure increase from 0 to 9 GPa, the two main peaks have moved to a lower energy region from 6.08 to 5.92 eV and 8.35 to 8.21 eV, respectively.

The optical properties of materials can be described by the refractive index and the extinction coefficient, and are closely related to dielectric constant. The refractive index and the extinction coefficient have also been calculated for chrysene under 0, 3, 6, and 9 GPa as displayed in Figure 7(c,d), respectively. The $k(\omega)$ shows a main peak at around 4.91 eV and

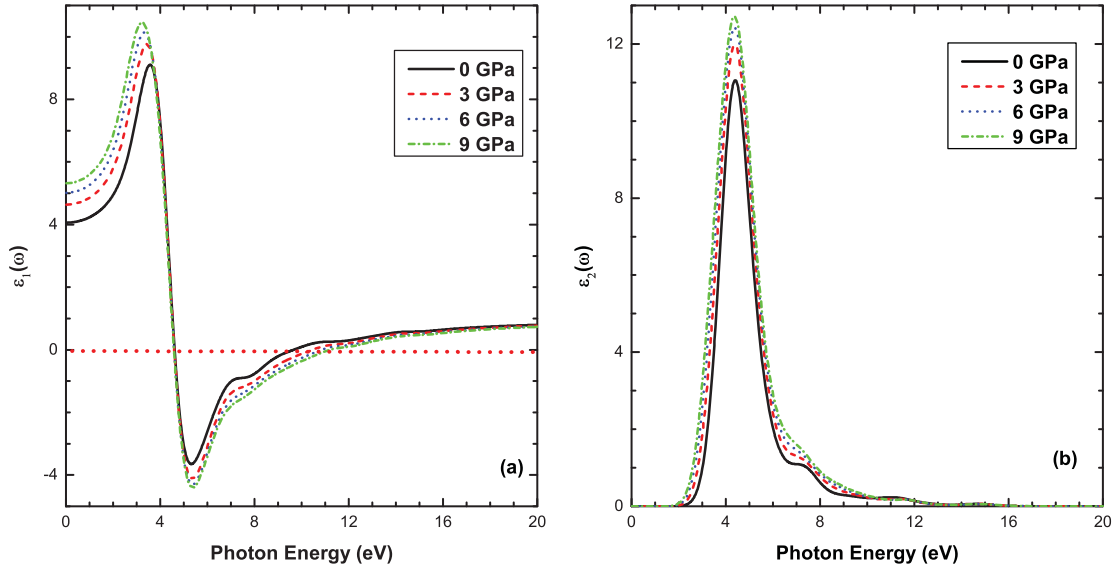

Figure 8. (Colour online) The dependence of the complex dielectric function of chrysene at 0, 3, 6, and 9 GPa, respectively. (a) The real part $\varepsilon_1(\omega)$ and (b) the imaginary part $\varepsilon_2(\omega)$.

4.89 eV for chrysene at 0 and 9 GPa, respectively. The peak intensity at around 4.91 eV is stronger than that at 4.89 eV. Both the refractive index and the extinction coefficient shift toward the lower-energy region when the pressure increases, which is consistent with the absorption coefficient ($\alpha(\omega)$) and reflectivity $R(\omega)$.

Meanwhile, the dielectric function is a crucial physical parameter describing the optical properties, and it reflects the linear response of materials to electromagnetic radiation. As shown in Figure 8(b), we notice there is a main peak at 4.36 eV in the $\varepsilon_2(\omega)$ spectrum of chrysene under no-pressure conditions. This peak takes its origin from the optical transitions between C 2p states in the conduction band. When the pressure increases from 0 to 9 GPa, the spectrum exhibits a small red shift without any notable shape changes. From Figure 8(a), the peaks of $\varepsilon_1(\omega)$ follow a similar trend of $\varepsilon_2(\omega)$ when applying an increasing pressure on chrysene. The zero frequency dielectric constant $\varepsilon_1(0)$ are found to be about 4.06, 4.64, 5.01 eV, and 5.32 eV at 0, 3, 6 and 9 GPa, respectively. Interestingly, it also can be seen from Figure 8(a), $\varepsilon_1(\omega)$ value is positive in the energy range of 4.61–9.38 eV, characteristic of semiconductor, while there is a broad peak around 5.27 eV below zero. The density of states shows that this phenomenon is caused by the electronic transition between the p orbital of carbon atoms and the 1s orbital of H atoms.

4. Conclusion

To extend our knowledge about the chrysene under pressure, we performed the first-principles method to study its electronic and optical properties. According to our work, we found that the optical properties of chrysene undergo a red shift with increasing pressure. Meanwhile, the pressure dependence of the electronic band structure, density of states and partial density of states of chrysene were presented. All in all, the band gap as well as the optical response of chrysene could be tunable by pressure.

Acknowledgments

Parts of the calculations were performed at the Center for Computational Science of CASHIPS, the ScGrid of Supercomputing Center, and the Computer Network Information Center of the Chinese Academy of Sciences.

Disclosure statement

No potential conflict of interest was reported by the authors.

References

[1] Forrest R. The path to ubiquitous and low-cost organic electronic appliances on plastic. Nature (London). 2004;428:911.
[2] Kelley W, Baude PF, Gerlach C, et al. Recent progress in organic electronics: materials, devices, and processes. Chem Mater. 2004;16:4413.
[3] Li G, Shrotriya V, Huang J, et al. High-efficiency solution processable polymer photovoltaic cells by self-organization of polymer blends. Nat Mater. 2005;4:864.
[4] Facchetti A. Semiconductors for organic transistors. Mater Today. 2007;10:28.
[5] Leising G, Tasch S, Brandstaetter C, et al. Red-green-blue light emission from a thin film electroluminescence device based on parahexaphenyl. Adv Mater. 1997;9:33.
[6] Aust B, Bentley WH, Drickamer HG. Behavior of fused-ring aromatic hydrocarbons at very high pressure. J Chem Phys. 1964;41:1856.
[7] Huang W, Zhong GH, Zhang J, et al. Constraint on the potassium content for the superconductivity of potassium-intercalated phenanthrene. J Chem Phys. 2014;140:114301.
[8] Kambe T, He X, Takahashi Y, et al. Synthesis and physical properties of metal-doped picene solids. Phys Rev B. 2012;86:214507.
[9] Burns M, Iball I. The bond lengths in chrysene. Acta Cryst. 1956;9:314.
[10] Roth, Mahns B, Schönfelder R, et al. Comprehensive studies of the electronic structure of pristine and potassium doped chrysene investigated by electron energy-loss spectroscopy. J Chem Phys. 2012;137:114508.
[11] Oehzelt M, Resel R. Nakayama A. High-pressure structural properties of anthracene up to 10 GPa. Phys Rev B. 2002;66:174104.
[12] Hummer K, Ambrosch-Draxl C. Electronic properties of oligoacenes from first principles. Phys Rev B: Condens Matter Mater Phys. 2005;72:205205.
[13] Kresse G, Furthmuller J. Efficiency of ab-initio total energy calculations for metals and semiconductors using a plane-wave basis set. Comput Mater Sci. 1996;6:15.
[14] Fedorov A, Zhuravlev YN, Berveno VP. Properties of crystalline coronene: dispersion forces leading to a larger van der Waals radius for carbon. Phys Status Solidi B. 2012;249:1438.
[15] Grimme S. Semiempirical GGA-type density functional constructed with a long-range dispersion correction. J Comput Chem. 2006;27:1787.
[16] Ilawe V, Zimmerman JA, Wong BM. Breaking badly: DFT-D2 gives sizeable errors for tensile strengths in palladium-hydride solids. J Chem Theory Comput. 2015;11:5426.
[17] Lee H, Park JH, Soon A. Assessing the influence of van der Waals corrected exchange-correlation functionals on the anisotropic mechanical properties of coinage metals. Phys Rev B. 2016;94:024108.
[18] Podeszwa, Rice BM, Szalewicz K. Predicting structure of molecular crystals from first principles. Phys Rev Lett. 2008;101:115503.
[19] von Lilienfeld A, Tkatchenko A. Anatole von Lilienfeld O. Two- and three-body interatomic dispersion energy contributions to binding in molecules and solids. J Chem Phys. 2010;132:234109.
[20] Monkhorst J, Pack JD. Special points for Brillouin-zone integrations. Phys Rev B. 1976;13:5188.
[21] Cai Q, Yin Z, Zhang MS. First-principles study of optical properties of barium titanate. Appl Phys Lett. 2003;83:2805.
[22] Saha, Sinha TP, Mookerjee A. Electronic structure, chemical bonding, and optical properties of paraelectric $BaTiO_3$. Phys Rev B. 2000;62:8828.
[23] Venturo A, Felker PM. Intermolecular Raman bands in the ground state of benzene dimer. J Chem Phys. 1993;99:748.
[24] Saigusa, Sun S, Lim EC. Size and excess vibrational energy dependence of excimer formation in naphthalene clusters. J Phys Chem. 1992;96:2083.
[25] Xiao P, Zeng Z, Chen XJ. Structural and electronic properties of solid naphthalene under pressure: density functional calculations. Eur Phys J B. 2016;89:142.
[26] Vinet, Smith JR, Ferrante J, et al. A universal equation of state for solids. J Phys C. 1986;19:L467.
[27] Sham J, Schlüter M. Density-functional theory of the energy gap. Phys Rev Lett. 1983;51:1888.
[28] Munoz, Kunc K. Structure and static properties of indium nitride at low and moderate pressures. J Phys Condens Matter. 1993;5:6015.
[29] Urbach. Urbach Franz The long-wavelength edge of photographic sensitivity and of the electronic absorption of solids. Phys Rev. 1953;92:1324.